

Synthesis and Analysis of Highly Efficient GDC20 as Electrolyte for IT-Sofcs Application

R. Gupta^{1*}, A. K. Mishra², M.R. Majhi³, M. Buchi Suresh⁴

^{1,3}Departement of Ceramic Engineering, Indian Institute of technology, Banaras Hindu University, Varanasi- 221 005, U.P., India

²Department of Metallurgical Engineering, National Institute of Technology Raipur, Raipur-492 010, C.G, India

⁴Scientist, Centre for ceramic processing, International Advanced Research Centre for Powder Metallurgy and New Materials, Hyderabad- 500 005, A.P, India

Abstract--*In quest of better and better cost effective performance of electrolyte used in intermediate temperature solid oxide fuel cell (IT-SOFC), we synthesized dense electrolyte samples of $Ce_{0.8}Gd_{0.2}O_{1.9}$ (GDC20) followed by dry pressing technique and observed excellent performance such as exponential enhancement in ionic conductivity in 600^oc-800^oc temperature range. We prepared our all samples that were sintered in range of 1350^oc to 1600^oc and found best relative density at 1550^oc. Density of samples varied from 87% (1660^oc) to 94% (1550^oc) and micro structural study revealed variation in grain size from 1.65 μ m (1350^oc) to 10.4 μ m (1550^oc). Dynamic light scattering (DLS) analysis showed particle size distribution of GDC20 powder (starting material) in range of 220nm -200 nm. Moreover XRD analysis directly showed the presence of cubic phases in sample. Electrolyte test was performed very accurately using impedance test in which we calculated ionic conductivity of electrolyte and found higher than previous reported values.*

Key words--Gadolinium-doped ceria $Ce_{0.8}Gd_{0.2}O_{1.9}$ (GDC), Impedance spectroscopy, Intermediate-Temperature SOFC, Microstructure, Ionic conduction, sintering.

I. INTRODUCTION

Solid oxide fuel cells (SOFC) have been the apple of the eyes of many scientists in industrial sector. In the recent years, SOFC is suggested as an excellent and promising energy storage technique due to its tremendous capacities to act as a potential replacement for many existing energy storage system and consequently opening new doors for new technologies par today's machines and equipment. Therefore it's become almost mandatory to expose SOFC in industrial area due to its high energy conversion efficiency, fuel flexibility and low pollutant [1-3]. SOFC's electrolyte synthesis technique and its operating temperature are those crucial parameters wherein all scientists are working [4]. Several experiments have been attempted by many scientists to figure out all associated problems related to cost effective synthesis technique and lowering the operating temperature. After many attempts scientists found out that low or intermediate operating (500^oc-800^oc) temperature is an effective operation guideline for SOFC rather than to operate in higher temperatures (above 1000^oc). This modification does not only enhance the efficiency of SOFC while also increases the long term reliability of cell. There are some previous reported techniques to

reduce the operating temperature such as decrease the electrolyte thickness [5-7], lessen the electrode polarization resistance [8-10] and using high ionic conductivity electrolyte like doped ceria [11-13]. It has been observed that thin film of electrolyte doped with Ceria gives higher ionic conductivity even at low temperature than Ytria-stabilized Zirconia based conventional electrolyte material [13]. Recently several process have been evolved to fabricate thin film of electrolyte such as dry pressing [14,15] spray coating [16], tape casting [17], magnetron sputtering [18], slurry spin coating [19]. For instance, Changjing Fu et.al [17] reported their work on aqueous based tape casting fabrication technique to fabricate large size (8cm X 8cm) Ni-GDC composite anode and observed maximum power density (909 W/cm²) around 650^oc. They observed low performance of cell below 650^oc due to unfavorable reaction kinetics at such low temperature. Furthermore Chan et.al [16] group also reported their work on dense GDC thin film electrolyte (10 μ m) on anode support. Starting material was synthesized by solid state reaction of ceria and gadolinia at sintering temperature 1450^oC and they achieved excellent cell performance at low temperature around 600^oc. The important breakthrough was done by Xia and Liu group [14]. They used cost effective dry pressing technique and achieved better cell performance at low temperature (600^oc). Y.D Zhen et.al [20] reported their work on IT-SOFC using nano sized GDC powder that was an effective innovation to reduce the sintering temperature. It has been accepted that dry pressing is cost effective technique to fabricate anode supported SOFC whereas proper densification of electrolyte sample developed via this method is still in doubt. Therefore we were also concern about this problem and tried to minimize it and succeeded to achieve very good densification (up to 94%). Thus as far as the performance and cost effectiveness concern, we achieved better electrolyte performance even exponential increment in ionic conductivity at 600^oc -800^oc range which is well documented here.

II. EXPERIMENTAL

A. Sample Preparation and Analysis

GDC20 powder was acquired from Cotter International, Mumbai with purity 99.5% and then particle size analyzed using DLS (Dynamic Light

Scattering) and subsequent graphs of intensity figure 1. The molecular formula of the acquired sample was $Ce_{0.8}Gd_{0.2}O_{1.9}$ which is commonly called as pure GDC or GDC20. For powder processing, GDC20 powder is mixed with 0.2 g of methyl cellulose (MC) that acts as a binder. Then resultant is ball milled in organic media. The final slurry is dried in oven at $80^{\circ}C$ and granulated to fine powder using agate mortar. Green samples of 10mm diameter are compacted and are sintered at temperatures range of $1350-1600^{\circ}C$. After sintering, density of the prepared sample was measured by applying Archimedes principle and we used ES223SM-DR Precisa density weigher to weigh all the samples. Samples were polished using the mounting technique followed by thermal etching which was carried out at temperature $50^{\circ}C$ below respective sintering temperature in .Mounting was done by mixing 7.5 gram of citofix powder of 30mm diameter and 5 gram of durofix-2 liquid in such a way that the samples remain on the surface. Gold ion sputtering was also done to make electrolyte surface conducting for Scanning electron microscope (SEM) analysis. Thus microstructures of samples were thoroughly analyzed.

B. Microstructure and XRD Analysis

Microstructure and Morphology of the electrolyte were examined by a scanning electron microscope (SEM). The phase of GDC20 electrolyte was examined with X-ray Diffractometer (XRD) using Cu-Ka radiation.

C. Electrolyte Test

For impedance spectroscopy the samples were coated with platinum paste and subsequently heated 10-15 minutes. After that we heated all samples in tubular furnace at $800^{\circ}C$ (maximum working temperature of IT-SOFC) for 12 hours. Later Impedance result of each sample was examined at different temperatures ($100^{\circ}C-800^{\circ}C$) and at each interval of $50^{\circ}C$ temperature the frequency was varied from $1e^7$ hertz to 0.1 hertz. Using these data ionic conductivity and power density of each sample were calculated and analyzed.

III. RESULT AND DISCUSSION

A. Powder Analysis

Particle size distribution in bulk sample of GDC20 was analyzed by Dynamic light scattering (DLS) technique in which the process involves the study of all scattered signals by the particles of the materials. In course of analysis we plotted a graph of scattered light intensity against the diameter of particles as shown in fig 3.1. In this graph we can easily see that majority of well defined intensity of scattered light at 220nm with 97.6% intensity. This observation simply indicates the uniformity of powder as well as the diameter of particles that is approximately 220nm. Better is the uniformity of raw material results better sinter ability of the material and due to this fact our raw material has better chance to perform accurate and controlled subsequent sintering process.

B. Density Measurement

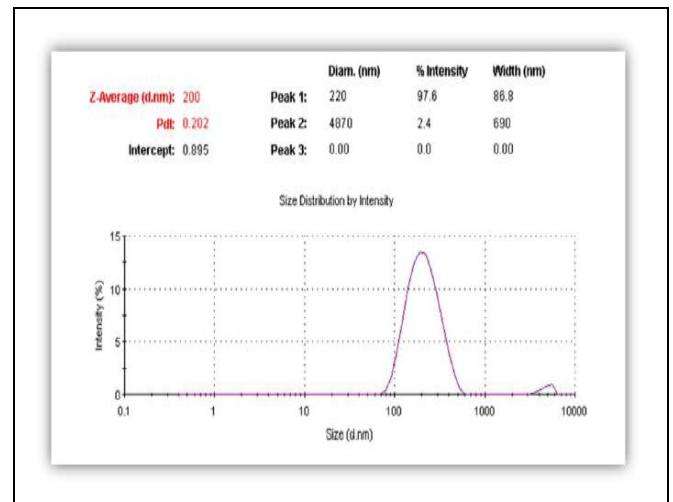


Fig 1, Shows size distribution with intensity

The Relative density of $1350^{\circ}C$, $1400^{\circ}C$, $1550^{\circ}C$, and $1600^{\circ}C$ sintered samples are calculated and found 88.95%, 89.77 %, 94 %, and 87.1 % respectively (figure 2) .Graph is plotted to depict the exact visualization what we found in experiment. In this graph variation in relative density with respect to sintering temperature is shown, in which slope of graph initially increases (in range of $1350^{\circ}C - 1550^{\circ}C$) and then suddenly decreases at $1600^{\circ}C$. Densification is found to be highest for $1550^{\circ}C$ that can be considered as a crucial sintering temperature. Explication for sudden decrement in densification includes reason such as the non uniformity in grain formation, uncontrolled grain boundary migration and amorphous nature of particle due to somehow oxidation at such higher temperature that causes less densification instead of increase in densification as we were expecting according to earlier pattern.

C. X- ray diffraction analysis

Figure 3 shows x-ray diffraction pattern for GDC20 sample sintered at $1550^{\circ}C$.It reveals the presence of crystalline cubic phases with crystal orientation such as (111), (200), (220), (311), (222), (400), (331), (420).The indices of these peaks are either even or odd that strongly means the presence of cubic phases. Crystalline behaviour of sample suggests the success of dry pressing technique.

D. Microstructure analysis

Figure 4(a) shows the microstructure of $1350^{\circ}C$ sample. Grain boundaries are clearly visible with hexagonal edges. Only one type of grain growth is observed here with mean grain size $1.65 \mu m$. Figure 4(b) shows the microstructure of $1400^{\circ}C$.It shows increment in relative density (from 88.95% to 89.77 %) as well as in grain size (from $1.65 \mu m$ to $3.57 \mu m$). $1550^{\circ}C$ sintered sample's microstructure is shown in figure 4(c) where grain growth is easily visible as expected. In this image

spherical pores are also visible. The average grain size of electrolyte sample at this temperature is 10.4 μm . In figure 4(d), strange behaviour of 16000c sintered sample is noted. After 15500c abnormal grain growth is found which is normally known as exaggerated grain growth. In this context coarsening of grain is take place where some larger grain grows unusually very quickly in matrix as compare to finer ones that leads to formation of bi-modal grain growth instead of uni-modal grain growth. Some rods like flakes are clearly visible which directly support our above explanation.

E. Sintering temperature Vs. Grain size

Figure 5 shows the variation in grain size against sintering temperature. From this graph we can easily interpret that how sintering temperature affects the grain growth. Decrease in slope is easily visible in this graph that indicates the unusual behaviour of grain after particular temperature range. As SEM images shows rod like flakes in microstructure. This abnormal visualization suggests further sintering process is not efficient because non-uniform particle size will not favour more densification if we follow the same.

F. Impedance Analysis

Figure 6 shows the various Cole-Cole plots of GDC20 sample (sintered at, 13000C, 14000C, 15500 C, 16000C for 2h) at different temperatures. Two semicircles were observed at lower temperatures. The high frequency semicircle contributes to grain conduction and low frequency semicircle to grain boundary conduction. As the working temperature is increased the impedance graph is shifted to the left indicating the decrease in the total resistance thereby giving significant increase in ionic conductivity in the intermediate temperature range of 6000C-8000C. From the graphs we can easily see that the diameter of semi circles are a function of working temperature and as the temperature increased, diameter of circles reduced and ultimately vanished. At high temperature, we found that only grain resistance is present which is also very small (due to the inductance caused by platinum wire). This trend is found to be similar for every sample in same range of operating temperature but for sample sintered at 15500c sample the total resistance was found to be minimum.

G. Electrolyte Performance

Figure 7 shows the variation in ionic conductivity against the working temperature. Conductivity was calculated from the total resistance of the sample at different temperatures. From figure 7 we can easily depict that the ionic conductivity is increased for all sample however it's found maximum for 15500c sample. This increase is significant especially at intermediate temperature region (6000c -8000c). The ionic conductivity for 15500c sintered sample is seems to be maximum due to its high concentration of stoichiometric defect.

IV. CONCLUSION

Dense GDC20 electrolytes were synthesized at different sintering temperatures at 1350⁰c, 1400⁰c, 1450⁰c, 1550⁰c and 1600⁰c. Maximum density is obtained in the sample sintered at 1550⁰c. Microstructures of the samples confirm that there is grain growth which is same for all of these samples except 1600⁰c. Microstructure of 1600⁰c sintered sample showed unusual flakes in precipitated form which seems like taken out from the parent matrix. In analysis we found that it was happened due to introduction of bi-modal grain growth. The ionic conductivity was found to increase exponentially with temperature. Thus with relative density, grain size, microstructure and impedance results we can conclude that the optimum sintering temperature for GDC20 electrolyte for IT-SOFC application is 1550⁰c. The ionic conductivity values are found to increase with the increase in working temperature. and are found to be better than reported value of other samples, indicating that GDC20 can be used as an electrolyte material for intermediate solid oxide fuel cell application. With low cost ceramic materials, cost effective fabrication technique and extremely high electrical efficiencies, SOFCs can deliver attractive economics.

V. ACKNOWLEDGEMENT

The authors would like to thank the centre for ceramic processing at International Advanced Research Centre for Powder Metallurgy and New Materials (ARCI), Hyderabad to provide all essential materials and instruments.

REFERENCES

- [1] Minh NQ. Ceramic fuel cells. J Am Ceram Soc 1993; 76:563–88.
- [2] Steele BCH. Materials for fuel cells. Nature 2001;414:345–52.
- [3] N.P. Brandon, S. Skinner, B.C.H. Steele, Annu. Rev. Mater. Res. 33 (2003) 183–213.
- [4] Koyama M, Wen C, Masuyama T, Otomo J, Fukunaga H, Yamada K, et al. The mechanism of porous Sm_{0.5}Sr_{0.5}CoO₃ cathodes used in solid oxide fuel cells. J Electrochem Soc 2001; 148:A795–801.
- [5] S. de Souza, S.J. Visco, L.C. de Jonghe, J. Electrochem. Soc. 144 (1997) L35–L37.
- [6] J.W. Kim, A.V. Virkar, K.Z. Fung, K. Mehta, S.C. Singhal, J. Electrochem. Soc. 146 (1999) 69–78.
- [7] J. Will, A. Mitterdorfer, C. Kleinlogel, D. Perednis, L.J. Gauckler, Solid State Ionics 131 (2000) 79–96.
- [8] C. Xia, M. Liu, Adv. Mater. 14 (2002) 521–523.
- [9] Z.P. Shao, S.M. Haile, Nature 431 (2004) 170–173.
- [10] S.P. Jiang, S. Zhang, Y.D. Zhen, W. Wang, J. Am. Ceram. Soc. 88 (2005) 1779–1785.
- [11] T. Ishihara, T. Shibayama, M. Honda, H. Nishiguchi, Y. Takita, J. Electrochem. Soc. 147 (2000) 1332–1337.

- [12] K. Huang, J.H. Wan, J.B. Good enough, J. Electrochem. Soc. 148 (2001) A788–A794.
- [13] B.C.H. Steele, Solid State Ionics 129 (2000) 95–110.
- [14] C. Xia, M. Liu, Solid State Ionics 144 (2001) 249–255.
- [15] C. Xia, M. Liu, J. Am. Ceram. Soc. 84 (2001) 1903–1905.
- [16] Y.J. Leng, S.H. Chan, S.P. Jiang, K.A. Khor, Solid State Ionics 170 (2004) 9–15.
- [17] Changjing Fu , Siew Hwa Chan, Qinglin Liu , Xiaoming Ge , G. Pasciak ,International Journal of hydrogen energy (2010) 301-307.
- [18] P.K. Srivastava, T. Quach, Y.Y. Duan, R. Donelson, S.P. Jiang, F.T. Ciacchi, S.P.S. Badwal, Solid State Ionics 99 (1997) 311–319.
- [19] N. Ai, Z. Lu, K. Chen, X. Huang, B. Wei, Y. Zhang, S. Li, X. Xin, X. Sha, W. Su, J. Power Sources 159 (2006) 637–640.
- [20] Y.D. Zhen, A.I.Y. Tok , S.P. Jiang b, F.Y.C. Boey. Journal of Power Sources 178 (2008) 69–74.

APPENDIX

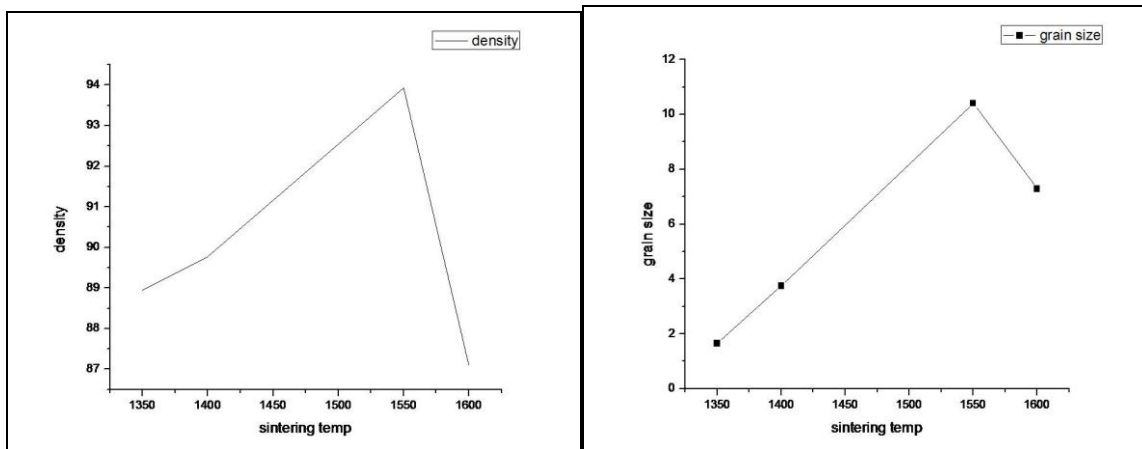


Fig 2&5, Shows the variation of relative density and grain size, respectively, with temperature.

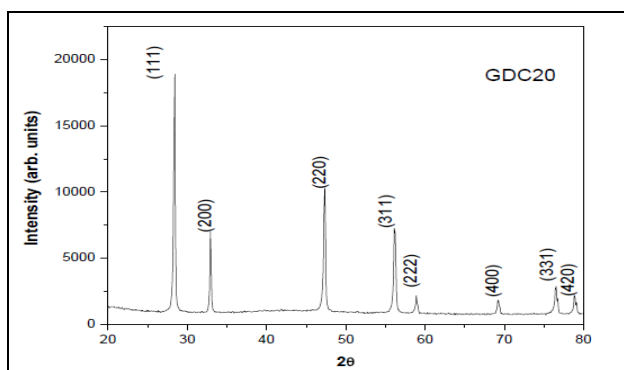


Fig 3, X-ray diffraction pattern of 1550^oc sintered GDC20 sample

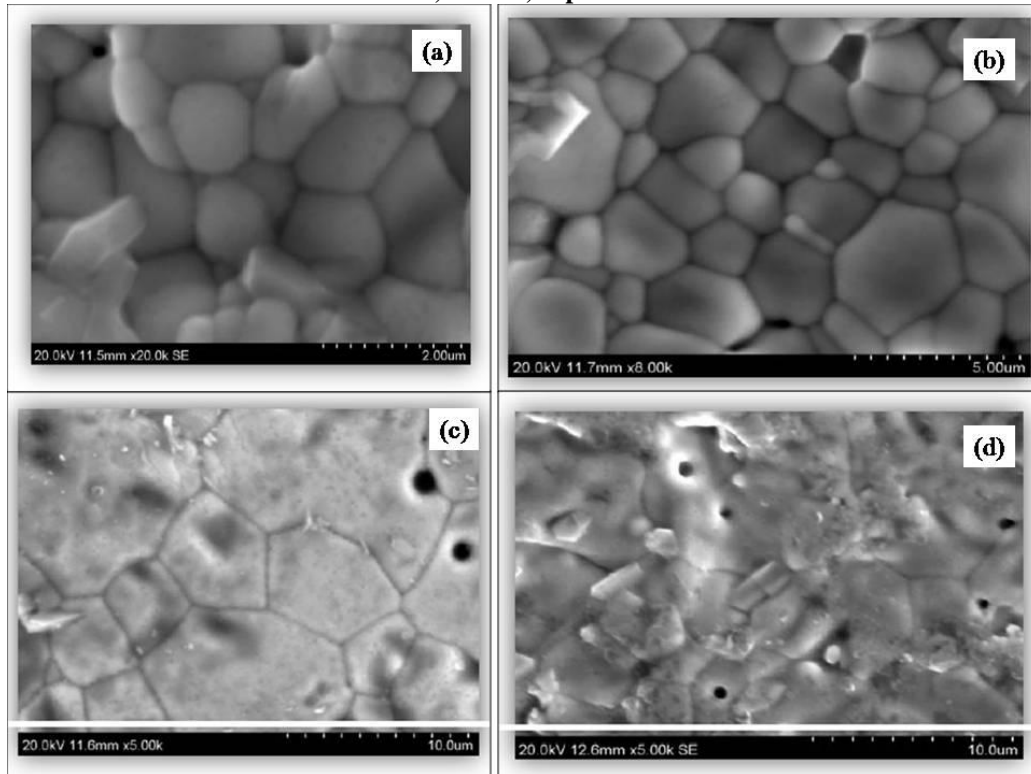
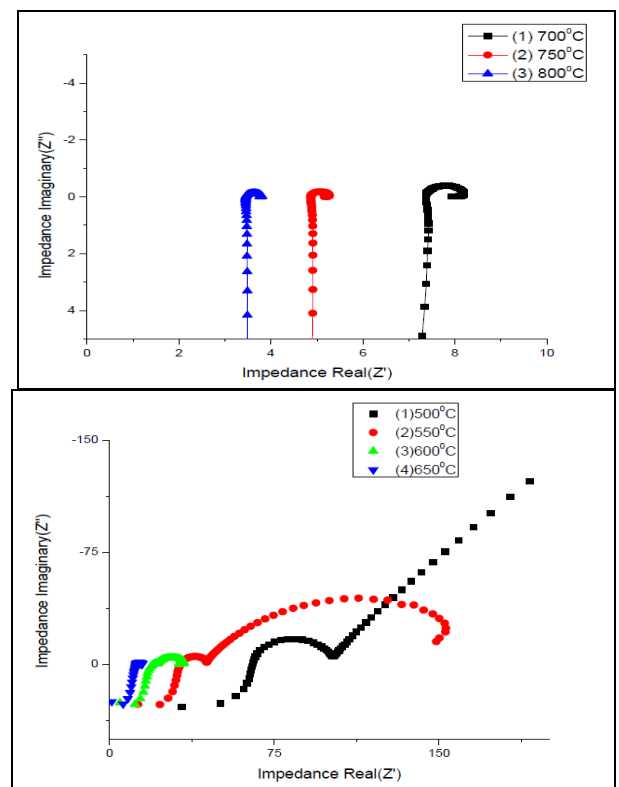
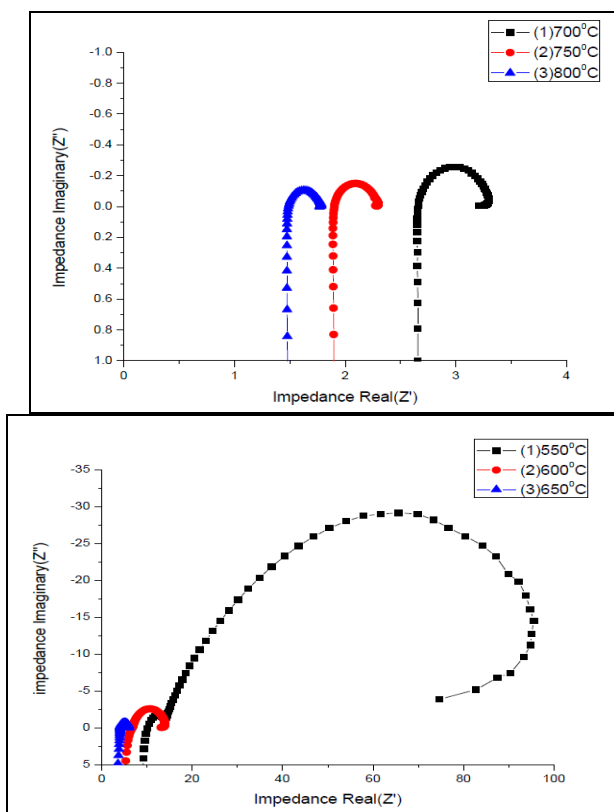


Fig 4, Shows the SEM images of sintered samples: (A)1350⁰C (B) 1400⁰C (C) 1550⁰C (D) 1600⁰C



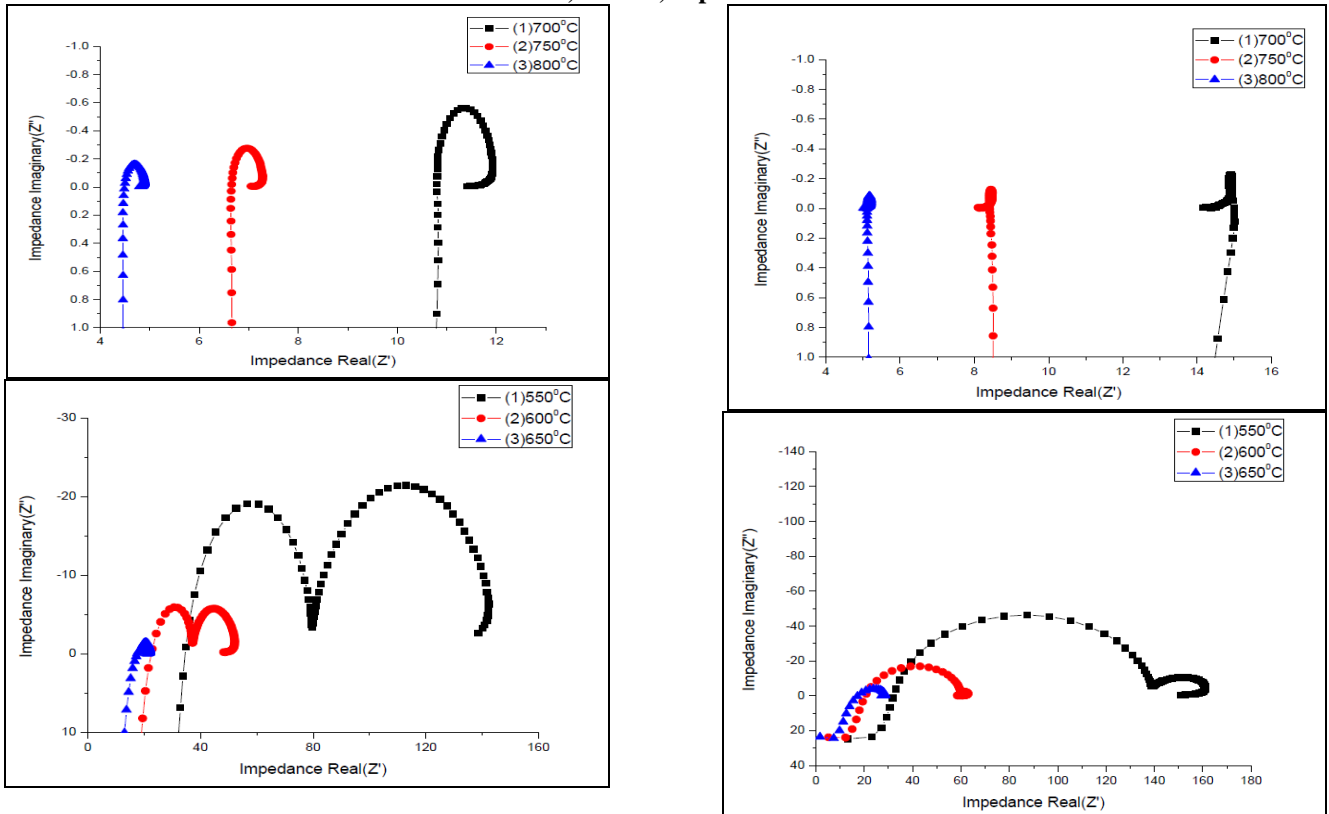


Fig 6, Cole-Cole plot of impedance analysis for 1350 °c, 1400°c, 1550°c, 1600°c samples

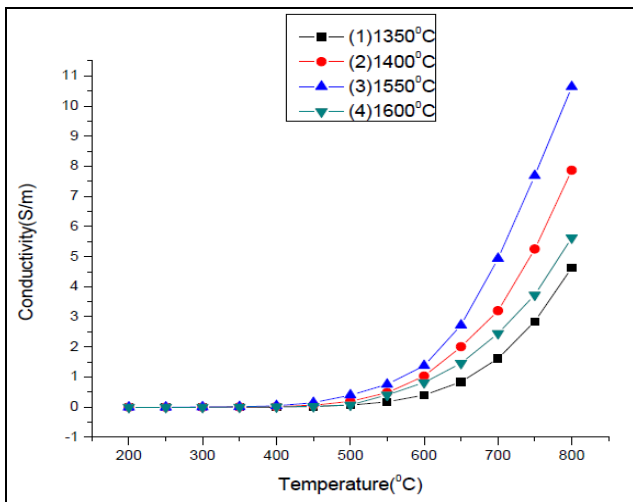


Fig 7, Ionic conductivity of electrolyte against working temperature for various samples